

Supplementary Figure Legends

Figure S1. (A) Viral load Ct value versus days after the estimated virus exposure for each patient. The viral clearance rate is defined as the slope, and patients were separated into fast and slow clearance groups.

(B) tSNE maps of abundances of NK cells with indicated characteristics for each patient. The maps are color coded by cell density (yellow is high, and purple is low). The numbers indicate the cluster IDs of each FlowSOM metacluster.

Figure S2. tSNE visualizations of median arcsinh-transformed intensities of markers in the CyTOF panel in each FlowSOM cluster. Red is high. Blue is low.

Figure S3. (A) The correlations between cell frequencies and the viral clearance in FlowSOM metaclusters that are not shown in Figure 1F.

(B) Representative biaxial contour plots of NKp46 and NKp30 from samples from patients in fast and slow clearance groups. The numbers indicate the percentage of cells in each quadrant.

(C) Boxplots of the frequencies of NKp30⁺ NKp46⁺ cells in patients from slow (n=10) and fast (n=11) groups in two independent experiments. Maximums, 75th, 50th, 25th percentiles, and minimums are 47.70, 39.05, 31.70, 15.90, and 14.00 for the slow group and 64.60, 51.30, 41.80, 28.80, and 12.50 for the fast group. *P*-value=0.0461 based on one-tailed unpaired Student's *t* test.

(D) Biaxial contour plots of DNAM1 and TIGIT from patients and healthy donors.

(E) Histogram overlays of percentage of the maximum events for DNAM1 and TIGIT in NK cells from two healthy donors vs. CyTOF intensity (left) and fluorescence intensity (right).

Figure S4. (A) Heatmap of pair-wise Pearson's correlation coefficients used to identify correlated markers in co-culture experiments. Positive correlations are displayed on a red scale, and negative correlations are displayed on a blue scale.

(B) Spearman correlations of pseudo-time point data (layers 1 to 10) based on TICONET vs. experimental data (Day 0 to Day 11) for the combined data for all three cell types (upper left), ectoderm (upper right), endoderm (lower left), and mesoderm (lower right).

(C) Heatmap of arcsinh-transformed marker intensities of protein expression (horizontal dimension) from the 0-hour time point NK cells in clusters C1 to C12 (vertical dimension).

(D) Line graphs of arcsinh-transformed intensities of the indicated markers from NK cells in each TICONET cluster. The cytolytic-skewed clusters are indicated by the green rectangle. The y-axis data are scaled marker intensities, and x-axis data are levels in each TICONET cluster.

(E) Boxplots of arcsinh-transformed intensities of 30 features obtained from TNFa-skewed (purple) and cytolytic-skewed (green) NK cells. Markers were sorted according to the adjusted *P* by Mann-Whitney U test after Bonferroni correction.

Figure S5. (A) Dot plots of the differential expression of ligands induced after pseudovirus infection of A549 cells (gray) and Calu-1 cells (black) in two independent experiments. Differential expression was calculated by subtracting the arcsinh-transformed intensity of ligands in cells that do not express the viral spike protein from that in the cells that do express the spike protein. Data represent mean ± SEM.

(B) Representative immunofluorescence images of a lung tissue section from a SARS-CoV-2-infected patient stained for nectin-4 (red) and N protein (green). Cell nuclei were visualized with DAPI (white).

(C) The hierarchical manual gating strategy for different cell types in PBMCs samples.

(D) Histogram overlay of DNAM1 and TIGIT expression on NK cells with or without IL-2 treatment overnight. Gray line represents the fluorescence-minus-one (FMO) control; black line and orange line are data without and with IL-2 treatment, respectively.

(E) Histogram overlay of expression of IL-2 receptor subunits, CD25, CD122, and CD132 on NK cells with high or low DNAM1 expression. Gray line represents the FMO control; dark blue line and light blue are data for NK cells that express high and low levels of DNAM1, respectively.

(F) The heatmap of arcsinh-transformed protein expression of the NK receptor on the NK cells expanded with K562-41BBL-mbIL-15 on Day 0 and Day 7.

Figure S1: Related to Figure 1.

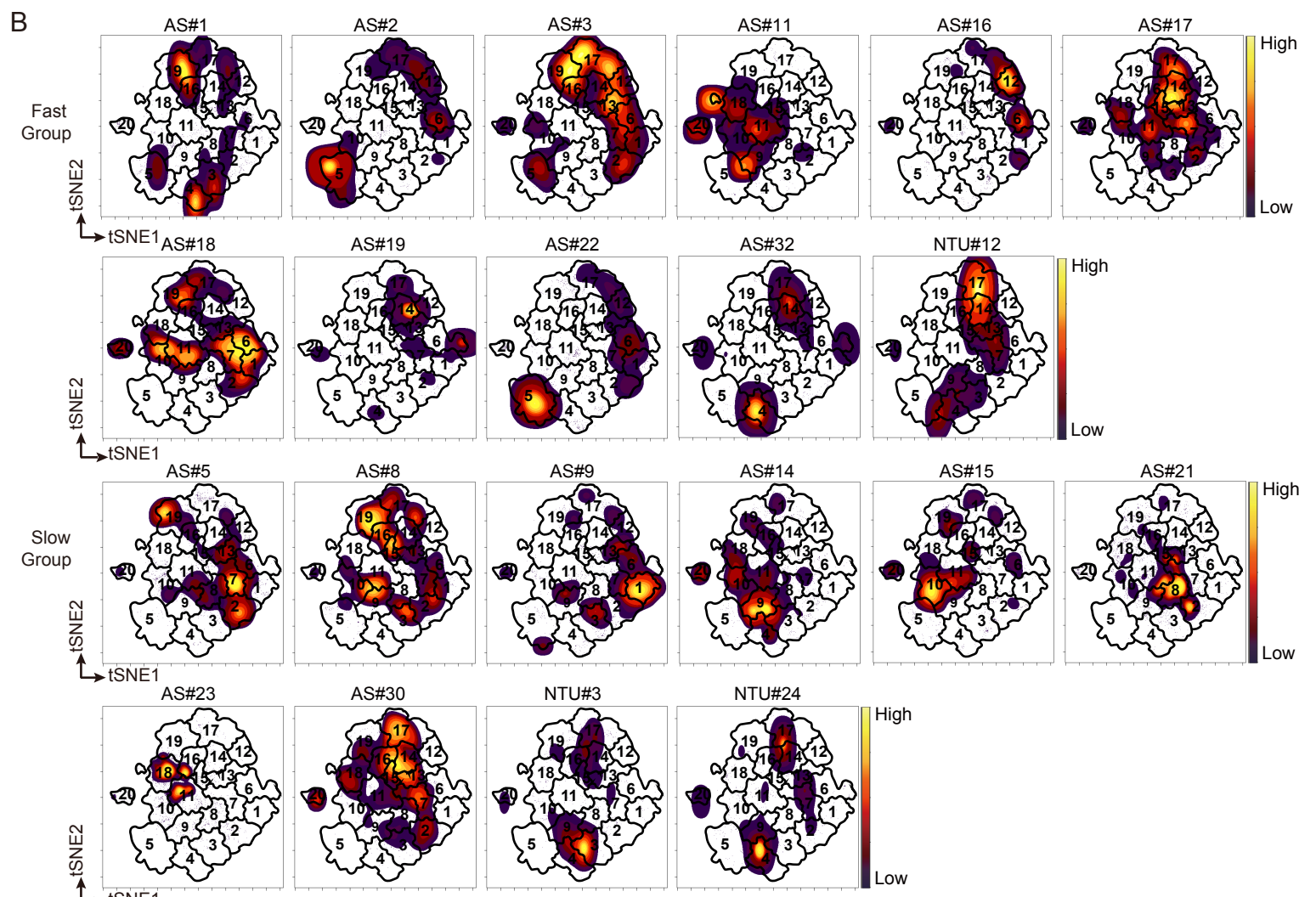
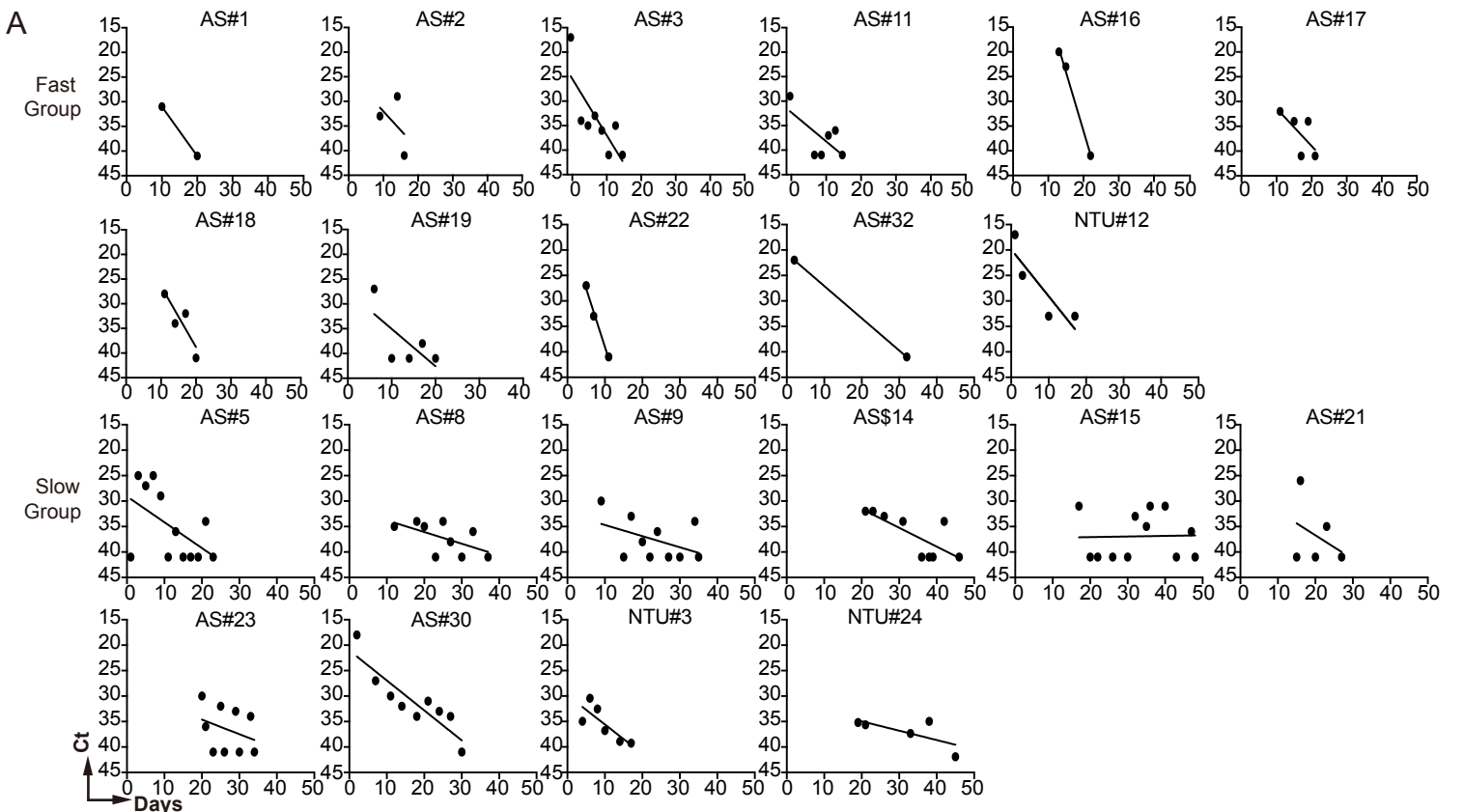


Figure S1. (A) Viral load Ct value versus days after the estimated virus exposure for each patient. The viral clearance rate is defined as the slope, and patients were separated into fast and slow clearance groups. (B) tSNE maps of abundances of NK cells with indicated characteristics for each patient. The maps are color coded by cell density (yellow is high and purple is low). The numbers indicate the cluster IDs of each FlowSOM metacluster.

Figure S2: Related to Figure 1.

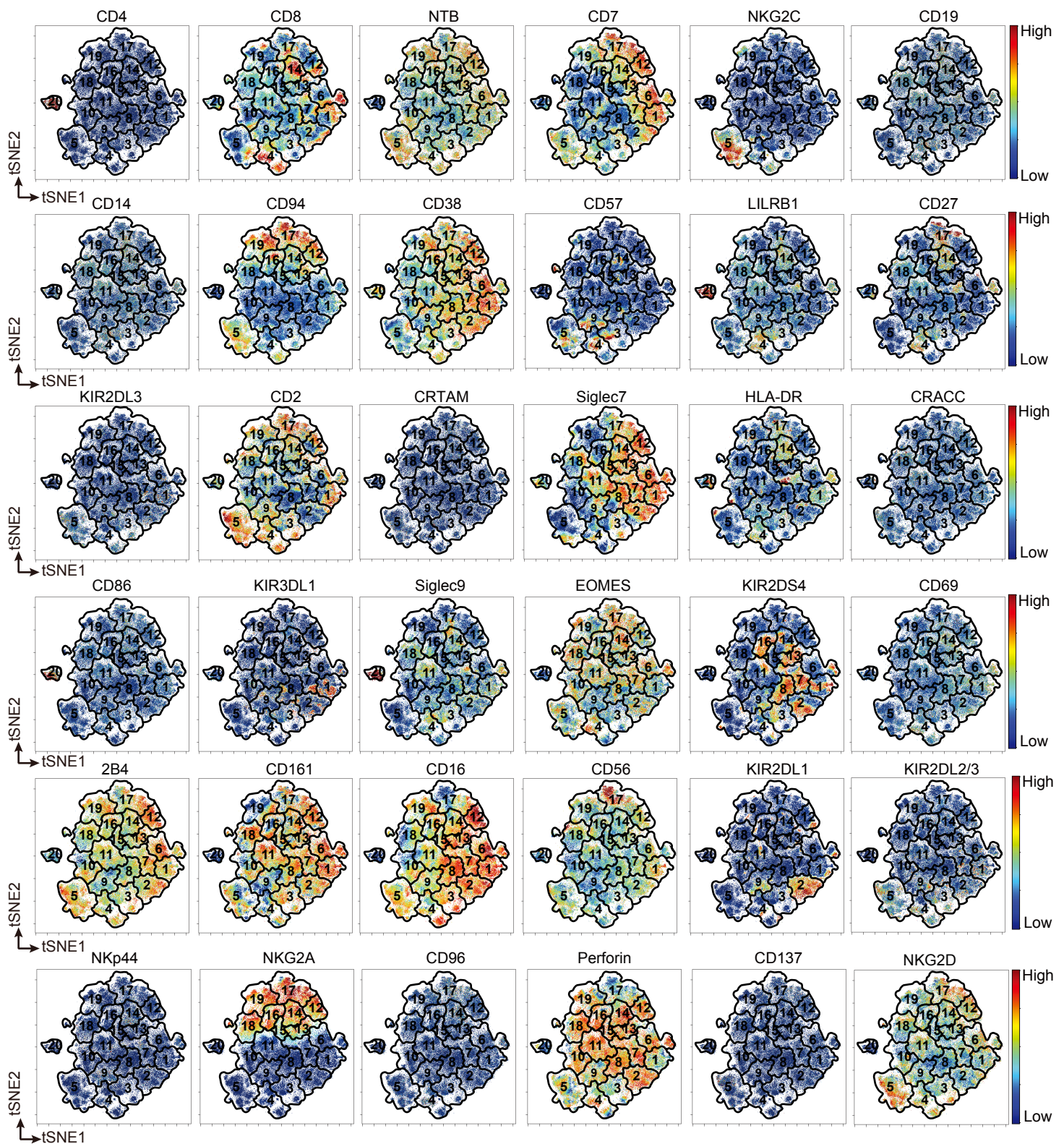


Figure S2. tSNE visualizations of median arcsinh-transformed intensities of markers in the CyTOF panel in each FlowSOM cluster. Red is high. Blue is low.

Figure S3: Related to Figure 1.

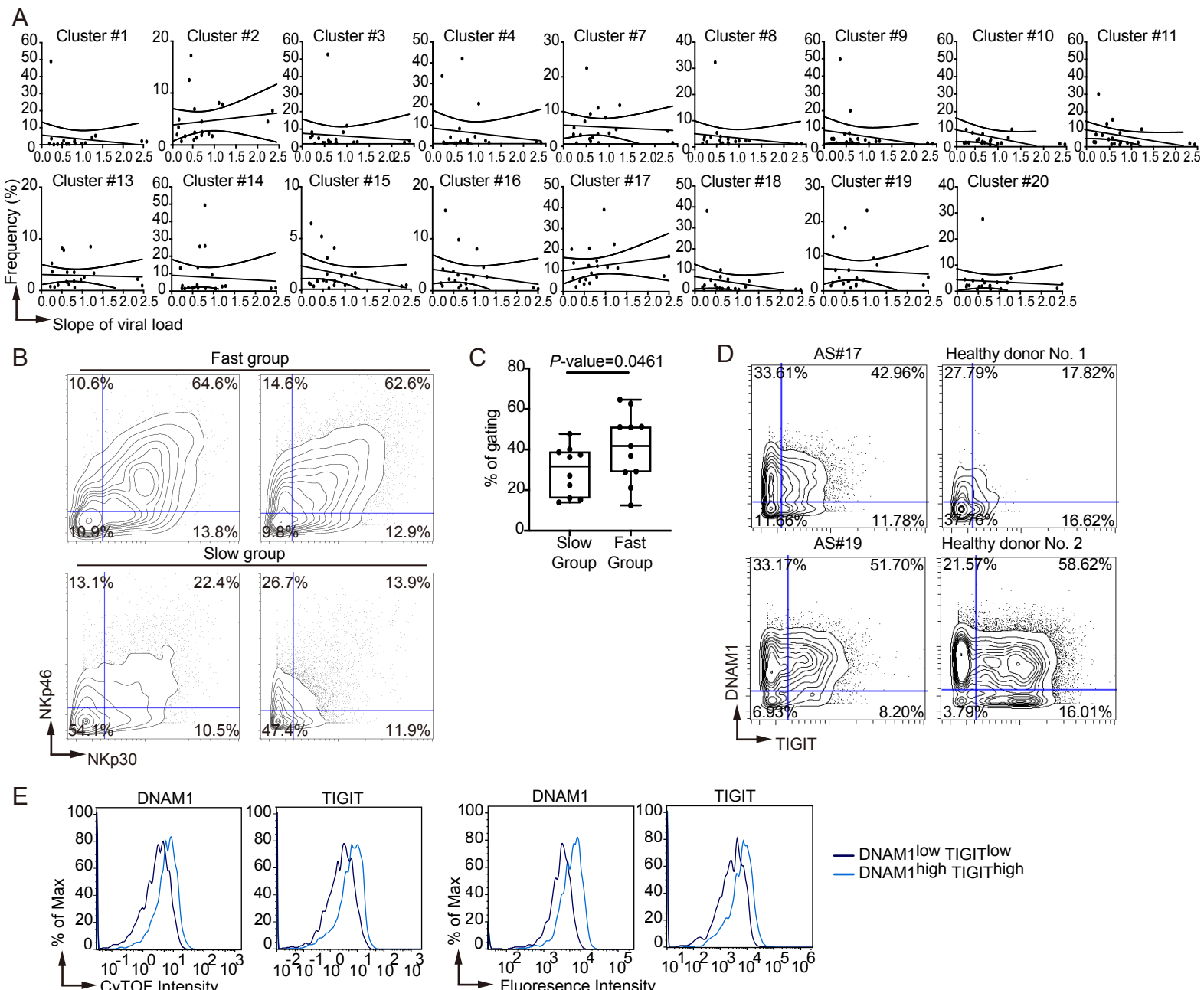
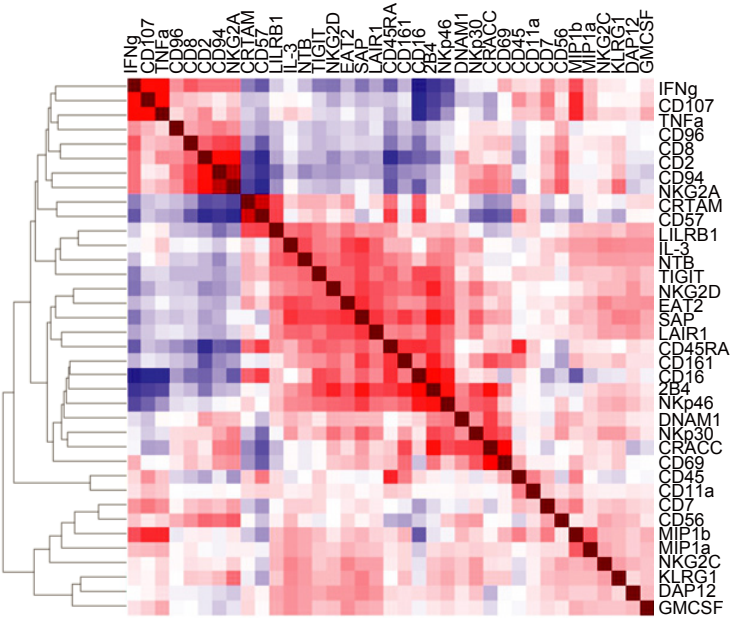


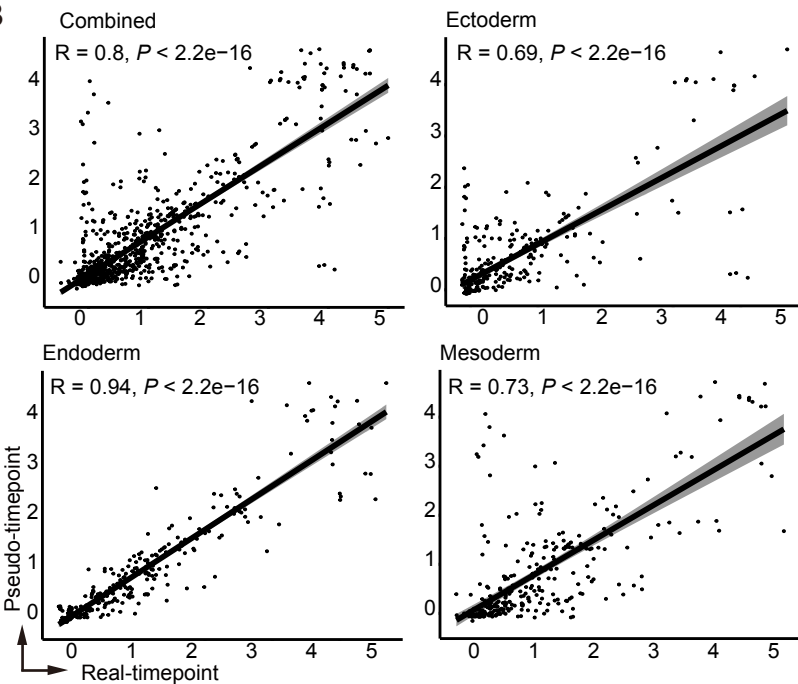
Figure S3. (A) The correlations between cell frequencies and the viral clearance in FlowSOM metaclusters that are not shown in Figure 1F. (B) Representative biaxial contour plots of NKp46 and NKp30 from samples from patients in fast and slow clearance groups. The number indicates the percentage of cells in each quadrant. (C) Boxplots of the frequencies of NK30+ NKp46+ cells in patients from slow (n=10) and fast (n=11) groups in two independent experiments. Maximums, 75th, 50th, 25th percentiles, and minimums are 47.70, 39.05, 31.70, 15.90, and 14.00 for the slow group and 64.60, 51.30, 41.80, 28.80, and 12.50 for the fast group. P-value=0.0461 based on one-tailed unpaired Student's t test. (D) Biaxial contour plots of DNAM1 and TIGIT from patients and healthy donors. (E) Histogram overlays of percentage of the maximum events for DNAM1 and TIGIT in NK cells from two healthy donors vs. CyTOF intensity (left) and fluorescence intensity (right).

Figure S4: Related to Figure 2.

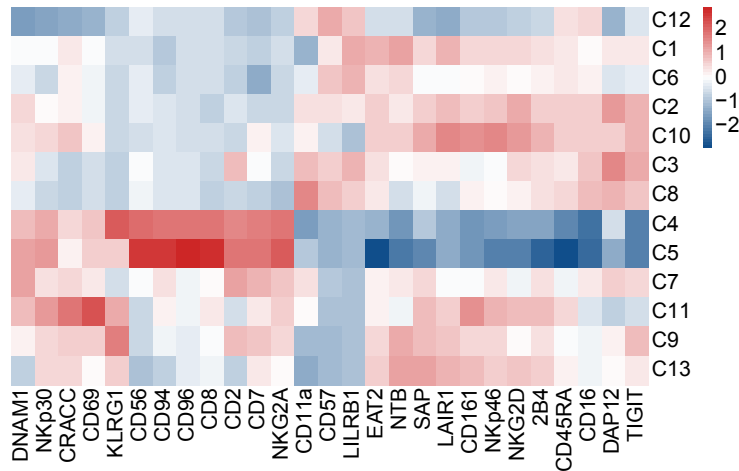
A



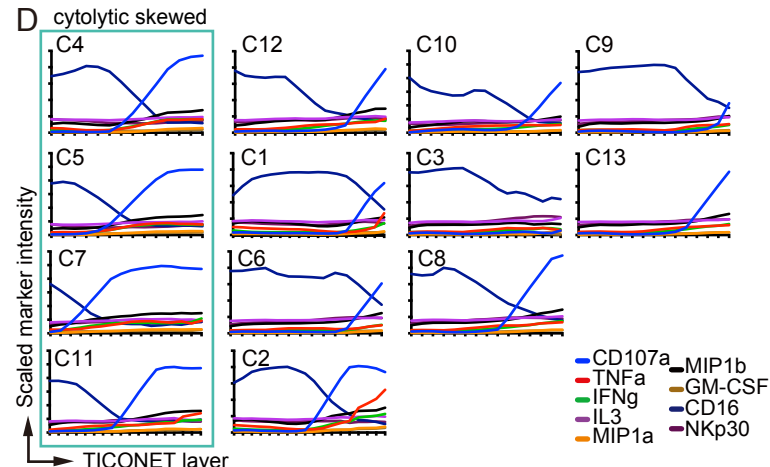
B



C



D



E

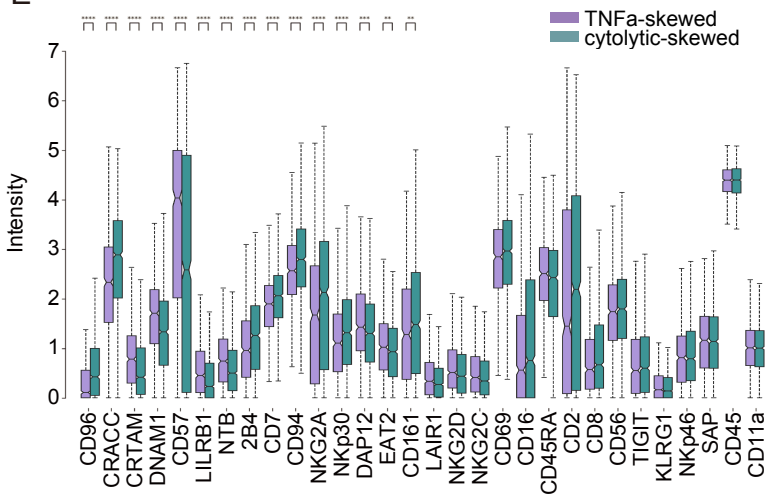


Figure S4. (A) Heatmap of pair-wise Pearson's correlation coefficients used to identify correlated markers in co-culture experiments. Positive correlations are displayed on a red scale, and negative correlations are displayed on a blue scale. **(B)** Spearman correlations of pseudo-time point data (layers 1 to 10) based on TICONET vs. experimental data (Day 0 to Day 11) for the combined data for all three cell types (upper left), ectoderm (upper right), endoderm (lower left), and mesoderm (lower right). **(C)** Heatmap of arcsinh-transformed marker intensities of protein expression (horizontal dimension) from the 0-hour time point NK cells in clusters C1 to C12 (vertical dimension). **(D)** Line graphs of arcsinh-transformed intensities of the indicated markers from NK cells in each TICONET cluster. The cytolytic-skewed clusters are indicated by the green rectangle. The y-axis data are scaled marker intensities, and x-axis data are levels in each TICONET cluster. **(E)** Boxplots of arcsinh-transformed intensities of 30 features obtained from TNFa-skewed (purple) and cytolytic-skewed (green) NK cells. Markers were sorted according to the adjusted P by Mann-Whitney U test after Bonferroni correction.

Figure S5: Related to Figure 3.

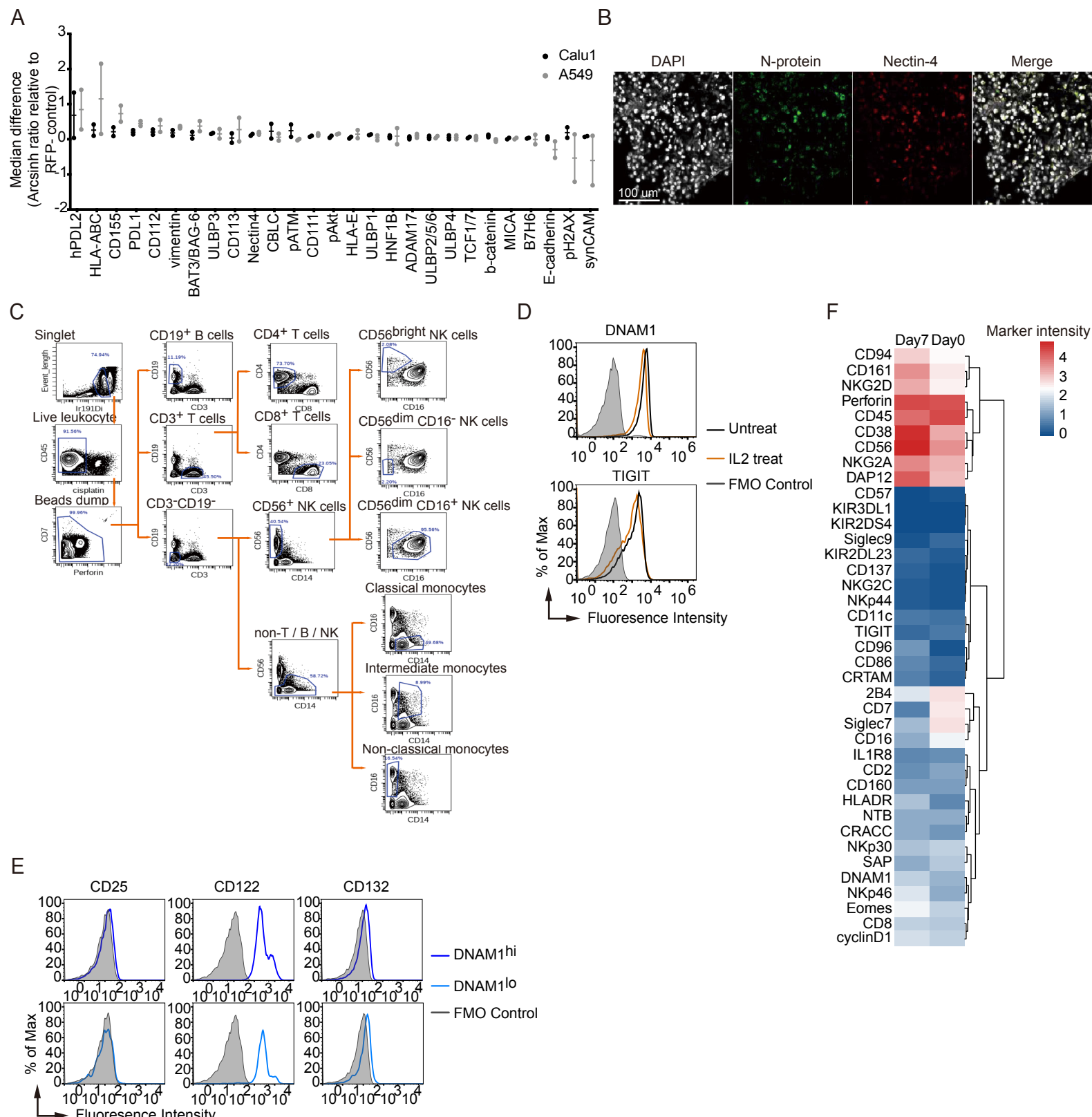


Figure S5. (A) Dot plots of the differential expression of ligands induced after pseudovirus infection of A549 cells (gray) and Calu-1 cells (black) in two independent experiments. Differential expression was calculated by subtracting the arcsinh-transformed intensity of ligands in cells that do not express the viral spike protein from that in the cells that do express the spike protein. Data represent mean ± SEM. (B) Representative immunofluorescence images of a lung tissue section from a SARS-CoV-2-infected patient stained for nectin-4 (red) and N protein (green). Cell nuclei were visualized with DAPI (white). (C) The hierarchical manual gating strategy for different cell types in PBMCs samples. (D) Histogram overlay of DNAM1 and TIGIT expression on NK cells with or without IL-2 treatment overnight. Gray line represents the fluorescence-minus-one (FMO) control; black line and orange line are data without and with IL-2 treatment, respectively. (E) Histogram overlay of expression of IL-2 receptor subunits, CD25, CD122, and CD132 on NK cells with high or low DNAM1 expression. Gray line represents the FMO control; dark blue line and light blue are data for NK cells that express high and low levels of DNAM1, respectively. (F) The heatmap of arcsinh-transformed protein expression of the NK receptor on the NK cells expanded with K562-41BBL-mbIL-15 on Day 0 and Day 7.

Table S1 The gender, age, and KIR and HLA genotypes of patients. Boxes indicate positive expression from the genotyping.

Subject ID	CENTROMERIC								TELOMERIC								KIR Ligand			
	3DL3	2DS2	2DL2	2DL3	2DL5B	2DS3/5	2DP1	2DL1	3DP1	2DL4	3DL1	3DS1	2DL5A	2DS3	2DS5	2DS1	2DS4	3DL2	HLA-A	HLA-B
AS1	---	---	---	---	---	---	---	---	---	---	---	---	---	---	---	---	---	BW4	BW6	C1/C1
AS2	---	---	---	---	---	---	---	---	---	---	---	---	---	---	---	---	---	BW4	BW4/BW6	C1/C1
AS3	---	---	---	---	---	---	---	---	---	---	---	---	---	---	---	---	---	BW6	---	C1/C1
AS5	---	---	---	---	---	---	---	---	---	---	---	---	---	---	---	---	---	BW4	---	C1/C1
AS8	---	---	---	---	2DS3	---	---	---	---	---	---	---	---	---	---	---	---	BW4	BW6	C1/C1
AS9	---	---	---	---	2DS3	---	---	---	---	---	---	---	---	---	---	---	---	BW6	---	C1/C1
AS15	---	---	---	---	---	---	---	---	---	---	---	---	---	---	---	---	---	BW4	---	C1/C1
AS16	---	---	---	---	2DS3	---	---	---	---	---	---	---	---	---	---	---	---	BW4	---	C1/C1
AS18	---	---	---	---	---	---	---	---	---	---	---	---	---	---	---	---	---	BW4/BW6	C1/C2	
AS21	---	---	---	---	---	---	---	---	---	---	---	---	---	---	---	---	---	BW4	---	C1/C1
AS22	---	---	---	---	2DS5	---	---	---	---	---	---	---	---	---	---	---	---	BW4	---	C1/C1
AS23	---	---	---	---	---	---	---	---	---	---	---	---	---	---	---	---	---	BW4	---	C1/C1
NTU3	---	---	---	---	2DS3	---	---	---	---	---	---	---	---	---	---	---	---	BW4/BW6	C2/C2	
NTU12	---	---	---	---	---	---	---	---	---	---	---	---	---	---	---	---	---	BW4/BW6	---	C1/C1
NTU24	---	---	---	---	2DS3	---	---	---	---	---	---	---	---	---	---	---	---	BW4	BW4	C1/C1
AS11	---	---	---	---	2DS3	---	---	---	---	---	---	---	---	---	---	---	---	BW4	BW6	C1/C1
AS14	---	---	---	---	---	---	---	---	---	---	---	---	---	---	---	---	---	BW4	BW4	C1/C1
AS17	---	---	---	---	---	---	---	---	---	---	---	---	---	---	---	---	---	BW4/BW6	---	C1/C1
AS19	---	---	---	---	---	---	---	---	---	---	---	---	---	---	---	---	---	BW4	BW6	C1/C1
AS30	---	---	---	---	---	---	---	---	---	---	---	---	---	---	---	---	---	BW4	BW4/BW6	C1/C1
AS32	---	---	---	---	---	---	---	---	---	---	---	---	---	---	---	---	---	BW4/BW6	---	C1/C1

 Framework gene
 Group A KIR gene
 Group B KIR gene

Table S2 Mass cytometry panel used for evaluation of COVID-19 patient peripheral blood.

Antigen	Clone	Metal label	Mass	Source	Catalog No.
CD45	HI30	Y	89	BioLegend	304002
CD3	UCHT1	In	113	BioXCell	BE0231
HLA-DR	L243	La	139	BioXCell	BE0306
CD7	CD7-6B7	Ce	140	BioLegend	343102
NKG2C	134591	Pr	141	R&D Systems	MAB138-100
CD19	HIB19	Nd	142	BioLegend	302202
CD14	M5E2	Nd	143	BioLegend	301843
CD94	DX22	Nd	144	BioLegend	305502
CD38	HIT2	Nd	145	BioLegend	303535
CD8	SK1	Nd	146	BioLegend	344727
LILRB1	292319	Sm	147	NOVUS	MAB20172
CD27	L128	Nd	148	BD	Custom
DNAM1	11A8	Sm	149	BioLegend	338302
KIR2DL3	180701	Nd	150	R&D Systems	MAB2014-SP
CD2	TS1/8	Eu	151	Fluidigm	3151003B
CRTAM	210213	Sm	152	R&D Systems	MAB16951-SP
Siglec7	6-434	Eu	153	BioLegend	339202
NTB	NT-7	Sm	154	BioLegend	317202
CRACC	162.1	Gd	155	BioLegend	331802
CD86	IT2.2	Gd	156	Fluidigm	3156035D
KIR3DL1	DX9	Gd	157	BD	555964
Siglec9	K8	Gd	158	BioLegend	351502
EOMES	WD1928	Tb	159	eBioscience	14-4877-82
NKp46	195314	Gd	160	R&D Systems	MAB1850-100
KIR2DS4	179315	Dy	161	R&D Systems	MAB1847-SP
CD69	FN50	Dy	162	BioLegend	310902
2B4	C1.7	Dy	163	BioLegend	329502
CD161	HP-3G10	Dy	164	BioLegend	339919
CD16	3G8	Ho	165	BioLegend	302051
NKG2D	ON72	Er	166	Fluidigm	3166016B
KIR2DL1	143211	Er	167	R&D Systems	MAB1844-SP
KIR2DL2/3	GL183	Er	168	Beckman	IM1846
NKp44	P44-8	Tm	169	BioLegend	325102
NKG2A	Z199	Er	170	Beckman	IM2750
CD96	NK92.39	Yb	171	BioLegend	338402
NKp30	210845	Yb	172	R&D Systems	MAB1849-SP
CD137	4B4-1	Yb	173	Fluidigm	3173015B
TIGIT	MBSA43	Yb	174	eBioscience	16-9500-82
Perforin	B-D48	Lu	175	Fluidigm	3175004B
CD56	NCAM16.2	Yb	176	BD	BDB559043
CD57	HNK1	Bi	209	BioLegend	359602
DNA		Ir	191/193	Fluidigm	201192A
Cisplatin		Pt	195	Sigma-Aldrich	P4394-100MG

Table S3 Mass cytometry panel for co-culture experiments

Antigen	Clone	Metal label	Mass	Source	Catalog No.
CD7	CD7-6B7	In	113	BioLegend	343102
CD45	HI30	In	115	BioLegend	304002
CD11a	HI111	La	139	BD Biosciences	14-0119-82
CD96	628211	Nd	142	R&D Systems	MAB6199-SP
CD107a	H4A3	Nd	143	BioLegend	328602
CD94	DX22	Nd	144	BioLegend	305502
IFNg	B27	Nd	145	BioLegend	506501
CD8	RPA-T8	Nd	146	Fluidigm	3146001B
CD57	HCD57	Sm	147	BioLegend	322302
CRTAM	210213	Nd	148	R&D Systems	MAB16951-SP
DNAM1	TX25	Sm	149	BioLegend	337102
MIP1b	D21-1351	Nd	150	Fluidigm	3150004B
CD2	TS1/8	Eu	151	Fluidigm	3151003B
TNF α	MAB11	Sm	152	Fluidigm	3152002B
CD45RA	HI100	Eu	153	Fluidigm	3153001B
NKG2D	1D11	Sm	154	BioLegend	320802
CRACC	162.1	Gd	155	BioLegend	331802
2B4	C1.7	Gd	156	BioLegend	329502
SAP	XLP 1D12	Gd	157	Cell Signaling	Custom
LAIR-1	DX26	Gd	158	BD Biosciences	550810
CD161	191B8	Tb	159	Beckman	Custom
NKp30	210845	Gd	160	R&D Systems	MAB1849-SP
DAP12	406288	Dy	161	R&D Systems	MAB5240-SP
CD69	FN50	Dy	162	Fluidigm	3162001B
EAT2	Polyclonal	Dy	163	Abcepta	AF1351a
GMCSF	BVD2-21C11	Dy	164	BioLegend	502301
CD16	3G8	Ho	165	Fluidigm	3165001B
TIGIT	MBSA43	Er	166	eBioscience	16-9500-82
IL-3	BVD8-3G11	Er	167	BioLegend	500502
NTB	NT-7	Er	168	BioLegend	317202
LILRB1	HP-F1	Tm	169	Beckman Coulter	Custom
NKG2C	134591	Er	170	R&D Systems	MAB138-100
MIP1a	93342	Yb	171	R&D Systems	MAB2701-SP
NKp46	195314	Yb	172	R&D Systems	MAB1850-100
NKG2A	Z199	Yb	174	Beckman	IM2750
KLRG1	2F1	Lu	175	eBioscience	562190
CD56	NCAM16.2	Yb	176	Fluidigm	BDB559043
DNA		Ir	191/193	Fluidigm	201192A
Cisplatin Viability		Pt	195	Sigma-Aldrich	P4394-100MG

Table S4 Mass cytometry panel for analysis of epithelial cells

Antigen	Clone	Metal label	Mass	Source	Catalog No.
vimentin	D21H3	In	113	Cell Signaling Technology	Custom
HLA-ABC	W6/32	La	139	BioLegend	311427
B7H6	875001	Pr	141	R&D Systems	MAB7144SP
synCAM	3E1	Nd	142	MBL	CM004-3
ULBP1	170818	Nd	143	R&D Systems	MAB1380-SP
ULBP3	166510	Nd	144	R&D Systems	MAB1517-SP
CD112 (Nectin-2)	TX31	Nd	145	BioLegend	337402
CD111 (Nectin-1)	R1.302	Nd	146	BioLegend	340402
B-catenin	D10A8	Sm	147	Fluidigm	3147005A
CD113 (Nectin-3)	N3.12.4	Sm	149	Santa Cruz Biotechnology	sc-69715
PDL1 (CD274)	E1L3N	Nd	150	Cell Signaling Technology	Custom
TCF1/7	C63D9	Eu	151	Cell Signaling Technology	Custom
pAkt (S473)	D9E	Sm	152	Cell Signaling Technology	Custom
ADAM17	111633	Eu	153	R&D Systems	MAB9301-SP
CD155	TX24	Sm	154	BioLegend	337502
BAT3/BAG-6	EPR9223	Gd	156	Abcam	ab137076
ULBP2/5/6	165903	Gd	157	R&D Systems	MAB1298-SP
E-cadherin (CD324)	67A4	Gd	158	BioLegend	324102
CBL-C	10F4.2	Tb	159	Millipore	MABS1173
Nectin-4	polyclonal	Gd	160	R&D Systems	AF2659-SP
pH2A.X (S139)	JBW301	Dy	161	Sigma-Aldrich	05-636
pATM (S1981)	EP1890Y	Dy	162	Abcam	ab81292
hPDL2 (CD273)	24F.10C12	Dy	163	BioLegend	329623
ACE2	polyclonal	Ho	165	R&D Systems	AF933-SP
ULBP4	709116	Er	166	R&D Systems	MAB6285-SP
HNF1B	polyclonal	Er	167	Proteintech	12533-1-AP
HLA-E	MEM-E/02	Er	168	Bio-Rad	MCA2193
N-Protein	36	Yb	172	Gift from Dr. An-Suei Yang	
MICA	159227	Bi	209	R&D Systems	MAB1300-SP
DNA		Ir	191/193	Fluidigm	201192A
Cisplatin Viability		Pt	195	Sigma-Aldrich	P4394-100MG